Proc. Fifth IFAC Symp. on Robot Control. Nantes, France, 1997. pp. 465--471

ADAPTIVE WINDOWING DISCRETE-TIME VELOCITY ESTIMATION TECHNIQUES: APPLICATION TO HAPTIC INTERFACES

Vincent Hayward, Farrokh Janabi-Sharifi, Chung-Shin Jason Chen

Department of Electrical Engineering and Center for Intelligent Machines
McGill University, 3480 University Street,
Montréal, PQ, Canada H3A 2A7
http://www.cim.mcgill.ca/~hayward/Home.html

Abstract: A method is described to estimate velocity from discrete and quantized position samples via adaptive windowing. It addresses the shortcomings of previously known methods which necessitate tradeoffs between noise reduction, control delay, estimate accuracy, reliability, computational load, transient preservation, and which cause difficulties with tuning. The method is optimal in the sense that it minimizes the velocity error variance while maximizes the accuracy of the estimates. The design of the estimator requires the selection of only one parameter, namely a bound on the noise. Simulation and experimental results are presented.

Keywords: Adaptive digital filters, Discrete time, Closed loop control, Computer interfaces, Estimation algorithms, PD controllers, Nonlinear filters, Velocity Measurements.

1 INTRODUCTION

On-line estimation of velocity from discrete time position signals is of considerable importance when velocity sensors are not available. Examples include velocity control of manipulators, visual servoing (Corke and Good, 1996), implementation of dissipative terms for force reflecting interfaces (Colgate and Brown 1994), and most guidance problems. In all these examples, velocity is used in the state feedback.

An adaptive windowing velocity estimation technique based on simple criteria and efficient for real-time applications is proposed in this paper in Section 3, 4, and 5. It addresses several difficulties associated with previous techniques such as finite difference and inverse-time methods, filtered derivative, alpha-beta trackers, and Kalman filtering, all of which are reviewed first.

Finite-difference methods use the Euler approximation to obtain a velocity estimate from discrete position measurements (Sinha et al. 1971). This method break down at high sampling rates when fine time-resolution is needed for feedback control. Inverse-time methods estimate of the velocity by dividing the interpulse angle from an encoder by the time between successive pulses (Habibullah et al. 1978). For a given a sampling period, the finite-difference method breaks down at low speeds and the inverse-time method breaks down at high speeds.

Filtering approaches are used to alleviate the difficulties associated with the noise amplification resulting from the differentiation of a noisy signal. Fixed low-pass filters can be applied to improve the estimates obtained by difference methods (Van Valkenburg 1960). For example, anti-aliasing analog filters can be applied to the position signal before it is sampled and quantized; digital filters can be used to smooth the velocity estimates, or both. In all cases, it is assumed that the position signal can be separated into spectral components: a low frequency component from which a velocity estimate can be reliably derived and a noisy component which must be filtered out. The design of fixed causal filters is constrained by fundamental tradeoffs between time lag, phase distortion, attenuation and cutoff precision. Typically, they need tuning for each application and operating condition, especially in closed loop since the filter becomes part of the system transfer function. A typical practical differentiator of the form (Lewis et al. 1993): $\hat{v}_k = \nu\hat{v}_{k-1} + (y_k - y_{k-1})/T$, with ν a design parameter, is known to cause resonance problems in closed loop. Here y_k and $\hat{v}_k$ are position measurement and velocity estimate at the kth instance, and T is the sampling period.

Alpha-beta trackers have also been proposed for optimal estimation of velocity from noisy position measurements (Lewis 1986). An alpha-beta tracker is a specialized form of double integrator Kalman filter. In (Glad and Ljung 1984), a Kalman filtering approach has been proposed for the velocity estimation based on position measurements obtained at irregular time instants. Further investigation has been done along this direction to optimize the Kalman filter performance for some models of signal generation (Bélanger 1992). But Kalman filtering assumes zero-mean Gaussian noise which is not always a valid assumption. For instance, the position measurement noise due to quantization is in fact better represented by a uniform distribution. Also, the convergence of Kalman filtering is not always guaranteed. The problem is addressed by limiting the effective memory of the filter using adaptive fading of past data using forgetting factors (Sorenson and Sacks 1971, Rao et al. 1993). It should be noted that the number of computations required per iteration is of order of n^3 for an n-th order Kalman filter, which will limit the rate when simple computational devices are used. Finally, tuning of the process noise covariance matrix is cumbersome and different operational conditions require tunings.

A final difficulty is shared by most of these methods. The signal is filtered the same way the noise is: rapid changes in the input signal will be attenuated, resulting in a poor transient response. In some applications such as that discussed in Section 5, preserving the transients is important.

In summary, all the existing methods share fundamental tradeoffs between:
i. noise reduction and control delay,
ii. accuracy of the estimate and reliability,
iii. computational load,
iv. difficulty of tuning,
v. preserving the transients.

2 VELOCITY ESTIMATION

Suppose a position signal $x(t)$ is sampled with period T. The true position at time kT is denoted by x_k. The position is measured with some error e_k such that

$$y_k = x_k + e_k. \tag{1}$$

e_k can be due to quantization (encoders, digital converters), calibration (systematic, cyclical), thermal noise, etc., and is usually assumed zero-mean white noise. In many situations, it is just as valid to assume that the error is simply bounded: $-d \le e_k \le d$. In the absence of additional information, the error can be considered to have a zero mean uniform distribution (in fact the case of pure quantization):

$$r = \mathrm{var}(e_k) = E[e_k^2] = \frac{d^2}{3} \tag{2}$$

The problem we consider is to produce an estimate $\hat{v}_k$ of $v(t) = dx(t)/dt$ from measurements $\{y_s\}_1^k$. The online solution of this problem for closed loop control applications imposes several requirements. The estimation algorithm has to reduce the effect of noise, and at the same time, minimize delay to avoid compromising the phase margin in closed loop control. These objectives are in conflict with fixed filters. In addition to producing reliable and accurate estimates, the technique should be computationally cheap. An effective estimation technique will allow the selection of larger control gains and hence yield lower tracking errors.

Achieving the objectives just stated: reduction of the effect of noise, minimization of delay, and minimizing computational cost for closed loop applications, is the focus of this paper. Conventional techniques for velocity estimation will be briefly discussed first in the rest of this section. We will then compare these algorithms with a newly introduced method via simulations and experiments.

2.1 Finite Difference Method

The finite difference method uses the Euler approximation for velocity estimation:

$$\hat{v}_k = \frac{y_k - y_{k-1}}{T} = \frac{x_k - x_{k-1}}{T} + \frac{e_k - e_{k-1}}{T} \tag{3}$$

This approach cannot result in accurate estimates at high sampling rates since the noisy component becomes correspondingly amplified.

2.2 Butterworth Filter

The effect of noise is reduced by a digital low-pass filter such as the commonly used Butterworth filter (Van Valkenburg 1960). The smoothing effect is achieved by forming a weighted sum of filtered and raw velocity estimates from the finite difference method, denoted by $\hat{v}_j$ and $\hat{v}'_j$ respectively,

$$\hat{v}_k = \sum_{j=0}^{n} b_j \hat{v}'_{k-j} + \sum_{j=1}^{n} a_j \hat{v}_{k-j}, \tag{4}$$

where a_j and b_j are the filter coefficients. As the order n of the filter increases, the filter approaches an ideal low-pass filter, but this will also cause larger time delays. Much effort must be put into the tuning of the cut-off frequency, furthermore the transients are suppressed.

2.3 Kalman Filter

Another approach is to describe the system by discrete stochastic dynamical equations and to apply Kalman filtering (KF) to these state equations (Glad and Ljung 1984, Bélanger 1992):

$$\mathbf{x}_{k+1} = A\mathbf{x}_k + G\mathbf{w}_k, \tag{5}$$

$$y_k = H\mathbf{x}_k + e_k, \tag{6}$$

Here $\mathbf{x}_k = (x_k, v_k, a_k)^T$, where a_k is the acceleration which could be dropped if double integrator model is used. A and H are the state transition and observation matrices:

$$A = \begin{bmatrix} 1 & T & T^2/2 \\ 0 & 1 & T \\ 0 & 0 & 1 \end{bmatrix}, \quad H = \begin{bmatrix} 1 & 0 & 0 \end{bmatrix}. \tag{7}$$

G is defined as the unity matrix for simplicity. $\mathbf{w}_k = [w_1, w_2, w_3]^T$ represents the process noise, which along with the measurement noise e_k is assumed to be zero-mean white Gaussian. The covariance matrix of $\mathbf{w}_k$, Q_k is

$$Q_k \delta_{kj} = E[\mathbf{w}_k \mathbf{w}_k^T] \tag{8}$$

where δ_{kj} is the Kronecker delta. The white noise $\mathbf{w}_k$ is viewed as a surrogate for either acceleration a (double integrator) or its derivative $\dot{a}$ (triple integrator) and therefore can be written as

$$Q_k = \mathrm{diag}[0, 0, q] \tag{9}$$

The wider the band of a or of $\dot{a}$ is, the better the stochastic model will represent the system. Since actual motions cannot be well characterized by a stationary random process, q must be taken as a parameter to be adjusted. The variance for the measurement error e_k is given by (2). The covariance matrix of measurement noise is a scalar r. The equations describing the discrete time Kalman filter are then

$$\begin{array}{lrcl} \text{Pred.:} & \hat{\mathbf{x}}_{k,k-1} & = & A\hat{\mathbf{x}}_{k-1,k-1} \\ & P_{k,k-1} & = & AP_{k-1,k-1}A^T + Q_k \\ \text{Gain:} & K_k & = & P_{k,k-1}H_k^T[r + H_k P_{k,k-1} H_k^T]^{-1} \\ \text{Update:} & \hat{\mathbf{x}}_{k,k} & = & \hat{\mathbf{x}}_{k,k-1} + K[y_k - H_k \hat{\mathbf{x}}_{k,k-1}] \\ & P_{k,k} & = & P_{k,k-1} - KH_k P_{k,k-1} \end{array} \tag{10}$$

In (Bélanger 1992), it is shown that the standard deviation of the velocity estimation error is 2-4 times better when the triple integrator model is used. The Kalman filter provides optimal (minimum variance, unbiased) estimation of state when the model is perfect. When the model is based on erroneous assumptions, however, the estimation might diverge. Adaptive fading Kalman filters have been proposed to help convergence (Fagin 1964, Rao et al 1993). A forgetting factor $\lambda_k \geq 1$ is introduced in the error covariance equation:

$$P_{k,k-1} = \lambda_k AP_{k-1,k-1}A^T + Q_k. \tag{11}$$

Since the performance critically depends on the selection of λ_k, an optimal and efficient algorithm for computing λ_k is used (Rao et al. 1993). The optimal forgetting factor can be computed as

$$\lambda_k = \max\{1, trace[N_k M_k^{-1}]\} \tag{12}$$

where

$$\begin{array}{rcl} M_k & = & H_k A P_{k-1,k-1} A^T H_k^T \\ N_k & = & H_k P_{k,k-1} H_k^T - H_k Q_k H_k^T \end{array} \tag{13}$$

3 ADAPTIVE WINDOWING

We now propose adaptive windowing techniques to address the issues raised by velocity estimation. To reduce the noise effect and hence to increase the accuracy, it was seen that the Euler approximation applied to two position samples is more precise if they are far apart. This observation is graphically conveyed by Fig. 1.

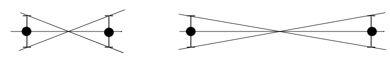

Figure 1: Effect of window length on the variance of velocity.

The larger the window length, the smaller the variance of the velocity will be. This is in fact equivalent to averaging the last n velocity estimates obtained from the finite difference method (3):

$$\hat{v}_k = \frac{1}{n}\sum_{j=0}^{n-1} \hat{v}_{k-j} = \frac{y_k - y_{k-n}}{nT} \tag{14}$$

Increasing the window size is equivalent to decreasing the sampling rate. A large window means larger delay and reduces the reliability of the estimation since it could miss intra-sample details.

In order to trade *precision* against *reliability*, the window size should be selected *adaptively* depending on the signal itself. The window size should be short when the velocity is high, yielding more reliable estimates and faster calculation; it should be large when the velocity is low so producing more precise estimates with negligible delays. The selection of the window size should be based on as little information as possible to preserve transients.

Noise reduction and accuracy put a lower bound on the window size, while reliability provides an upper limit for the window length. A reliability criterion is established to determine whether the slope of a straight line approximates reliably the derivative of the signal between two samples $x_k, \cdots, x_{k-n}$, it is then used to find the longest window which satisfies the accuracy requirement, solving a min-max problem.

A simple test is to check that the straight line between $y_k, \cdots, y_{k-n}$ passes through all intermediate samples given an uncertainty band defined by the peak norm of the noise

$$d = ||e_k||_\infty \forall k. \tag{15}$$

Estimates in the set $[\frac{x_k - x_{k-n}}{nT} - \frac{2d}{nT}, \frac{x_k - x_{k-n}}{nT} + \frac{2d}{nT}]$ are all possible, so a method must be found to select one optimally, since its existence is ensured constructively. How probable is any one of them? Combine (1) with (14):

$$\hat{v}_k - \frac{2d}{nT} \leq v_k \leq \hat{v}_k + \frac{2d}{nT}. \tag{16}$$

For a uniform noise distribution, this implies a triangular probability density function (PDF) for the velocity as on Fig. 2, with

$$\sigma_{v_k}^2 = \frac{2d^2}{3n^2T^2} \tag{17}$$

Hence, the slope of the line passing through y_k and y_{k-n} is the estimate of maximum likelihood. The maximum possible window size n will minimize the variance for the velocity error.

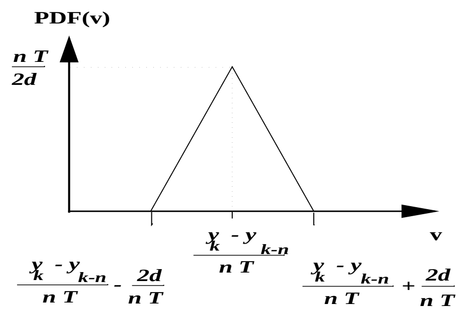

Figure 2: PDF of velocity for window of length n.

The estimator works as follows: at each time step, the maximum size of the window n which satisfies the reliability criterion is found and returns the slope of the line passing through y_k and y_{k-n}. We call this method *End-Fit First Order Adaptive Windowing* (End-fit-FOAW). From the above discussion, it follows that:

Proposition 1 *If a position trajectory has a piece-wise continuous and bounded derivative, and if the measurement noise is uniformly distributed, the proposed method minimizes the velocity error variance and maximizes the accuracy of the estimate.*

One way to introduce additional smoothing without loosing the advantages of the method is to produce a *best fit* estimate using all the samples in a window rather than an *end fit* based only y_k and y_{k-n} leading to a Best-fit-FOAW estimator. We could think of approaches similar to FOAW using higher order interpolations between samples (parabolic or higher), but these fall outside the scope of this paper.

The reliability criterion can be relaxed to account for the effects of outliers. An outlier is a rare event in the signal. Suppose that, for a given uncertainty band, an outlier occurs with probability p in a given time interval. Its effect on the estimator is to reset the window size, producing an inaccurate estimate with the same probability. A simple method to make the filter more robust is to stop the window growth only if two consecutive sample fall out of the fit. The probability for two outliers to occur in two consecutive samples is nearly p^2 which should be a very small number.

4 SIMULATION RESULTS

The comparison of performance between the proposed method and conventional techniques was undertaken. Evenly distributed noise ($\pm 5\%$) was added to a signal sampled at 100 Hz. The effect of a second order Butterworth filter with a 20 Hz cutoff frequency can be observed on Fig. 3 by comparison to plain FDM, where the noise is attenuated but the estimation lag is clearly seen.

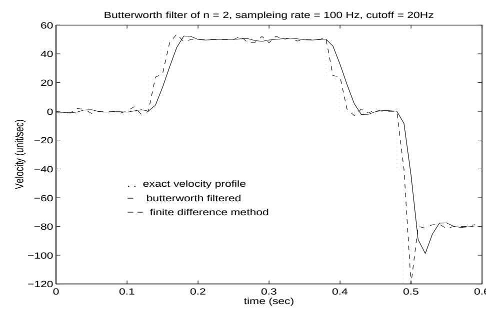

Figure 3: Comparison of exact velocity profile and FDM without and with Butterworth filter.

The End-fit-FOAW method was applied to the same position signal and its performance was compared with the FDM (Fig. 4). FOAW removes the velocity noise considerably with almost no time delay while preserving the transient parts of the signal. However, overshoot and undershoot is present in the estimated velocity signal.

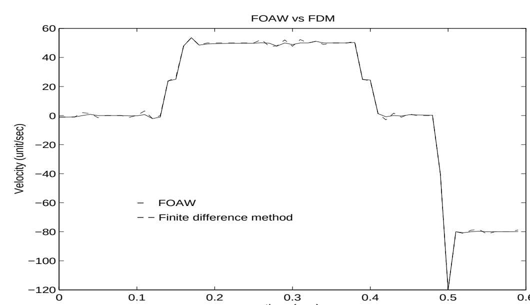

Figure 4: Comparison of finite difference method with End-fit-FOAW.

The Best-fit-FOAW improves the quality of the velocity estimation further as seen in Fig. 5.

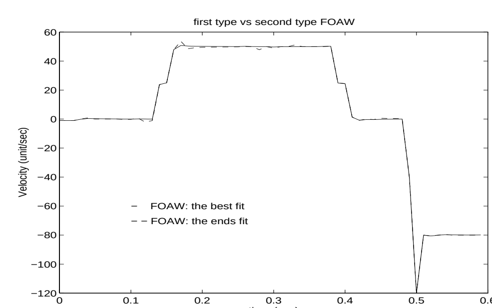

Figure 5: Comparison of the types of FOAW.

The performance of FOAW then was compared to that of adaptive fading Kalman filtering. The triple integrator model of (6), (7) was used and the system states were predicted and updated by equations (10). The variance r was calculated from (2). The velocity estimations are shown in Fig. 6, along with the FOAW-based estimations. q tuned for the best to tradeoff between delay and overshoot. It is seen that FOAW gives superior estimations in terms of delay and accuracy. Also, it should be noted that the Kalman filter tuned for this trajectory would not give equally good estimations for another trajectory.

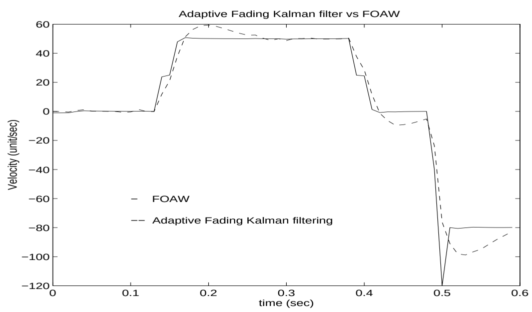

Figure 6: Comparison of the Best-fit-FOAW with Adaptive Fading Kalman Filtering.

5 EXPERIMENTAL RESULTS

One instance of the problem at hand is found in the rendering of virtual walls in the area of haptics. Minsky et al. (1990) found empirically that for virtual wall implementations (which is equivalent to high gain discrete PD control $Kx + B\dot{x}$, applied to an inertia) the stability condition s $B/(KT) > c$, where c is a constant found to be about 0.5. In (Bonneton, Hayward 1994), it was found using the Padé approximation that this constant is 2/3 if the digital loop has one delay and a zero-order-hold. This shows that if K is large, B must be large too. A noisy estimate of the velocity will limit B and therefore K as well. The generality of a haptic interface will depend largely on the freedom to select combinations of K and B gains.

A two-degree-of-freedom haptic device, the Pantograph (Hayward et al. 1994), is used in the experiment on achievable gains for K and B. The position signal is fed back to the input of a discrete time controller. The output is a torque command applied to a device which can be closely approximated by an inertia (very little friction and structural dynamics). The signal was purposely left quite noisy (not more than 8 stable bits out of 12).

Remember that, because it is a sampled data system, there exist several regimes of instability. For certain values of K and B, the system enters stable limit cycles, for other values, the system becomes unstable. The reported values reflect the onset of limit cycles and not diverging instabilities. The lower bound of the useful region is given by the amount of damping B that is required for each K to avoide a limit-cycle oscillatory behavior. The upper limit indicates the values of B which cause the noise to exceed a prescribed threshold for each K too. The interior composite region outlines the useful region—a region where gain selections are at the same time free of limit cycles and free of noise.

In the first three plots below, three velocity estimation techniques (FDM, End-fit-FOAW, and Best-fit-FOAW) are compared against each other, showing the effects of the sampling frequency on the system performance. In the three plots on the next page, the same data is presented in a different way. Each algorithm is studied for three different frequencies (300, 800, 1500 Hz).

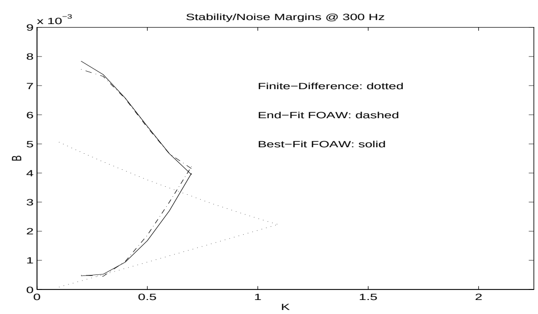

Figure 7: Stability-Noise regions for K and B with different estimation algorithms at 300 Hz.

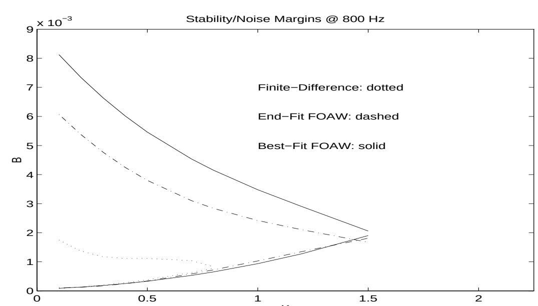

Figure 8: Same as above but at 800 Hz.

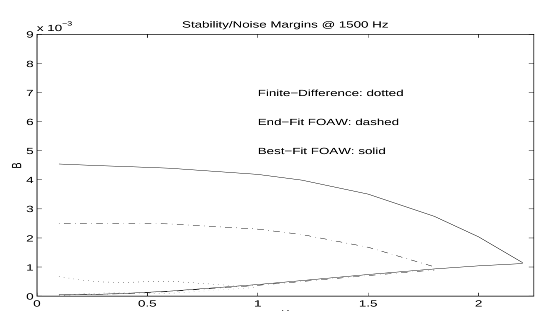

Figure 9: Same as above but at 1500 Hz.

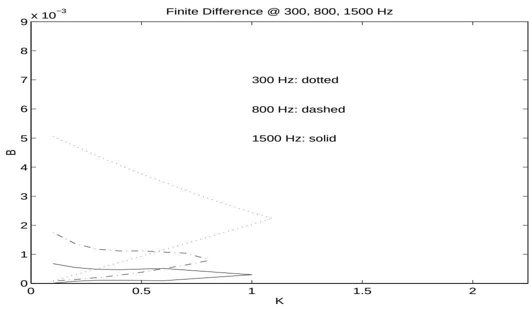

Figure 10: Stability-Noise regions for K and B for FDM at 300, 800, and 1500Hz.

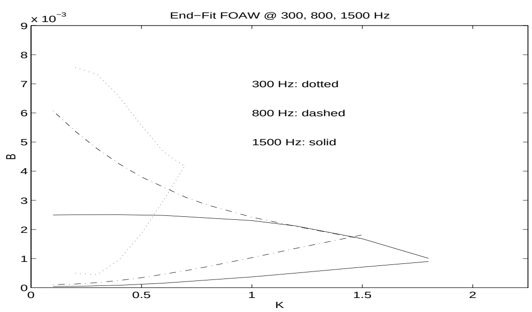

Figure 11: Stability-Noise regions for K and B with End-fit-FOAW at 300, 800, and 1500Hz.

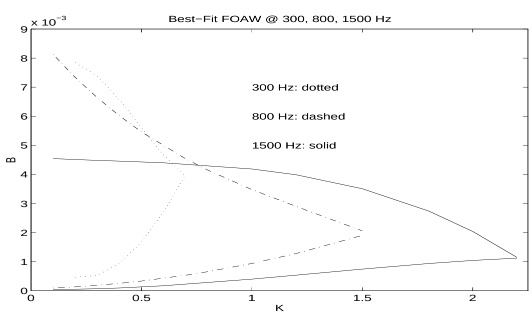

Figure 12: Stability-Noise regions for K and B for Best-fit-FOAW at 300, 800, and 1500Hz.

Several observations can be made:

1. Both FOAWs perform much better than FDM, especially when the sampling frequency is high. This is seen from the first three plots 7, 8, 9. FOAW estimators raise the upper limit of B for all K's with an exception for some K's at the lowest frequency, 300 Hz. This exception can be explained by the fact that FDM approximates the true velocity well enough at low sampling rates.

2. For any sampling rate, these regions are enlarged with the use of FOAW estimators (with the largest area for the *Best-Fit FOAW*. This, in essence, shows the effectiveness of the FOAW algorithms.

3. FOAW estimators yield an effective rejection of noise, and therefore result in a higher upper value of B, as compared to FDM. It also makes the system less susceptible to noise, especially at high frequencies, as shown in the flattening of upper bound B at 1500 Hz in the three plots 10, 11, 12.

4. FOAWs do not introduce instabilities due to delay since the lower limits of the composite regions remain unchanged at a fixed sampling frequency as in plots 8, 9.

5. The lower bound of the useful region is lowered with increasing sampling rates which demonstrates the necessity of better estimators to combat the effects of noise as seen in plots 10, 11, 12.

6 CONCLUSION

It was said in the introduction that finite-different methods break down at low velocities (resp. high rates) while inverse-time methods break down at high velocities (resp. low rates). FOAW adapts to the signal so at low velocities it resembles the inverse-time method since it measures the intervals between events which are far apart in time but close in space, while at high velocities it resembles the finite-difference method since it measures events which are far apart in space but close in time. Correspondingly, FOAW can also be viewed as an adaptive decimation technique. FOAW can also be considered from the view point of its transfer functions. When the velocity is high it is a filter of minimum order and when it is low it is a filter of maximum order which is lower pass.

7 ACKNOWLEDGMENTS

The authors would like to thank Professor Randy Ellis from Queen's University and Professor Dinesh K. Pai from the University of British Columbia for very stimulating initial discussions. The authors would also like to thank Hossein Najaf-Zadeh and Nader Sheikholeslami from the digital signal processing group at McGill University for their helpful comments.

Funding was provided by the project "Haptic Devices for Teleoperation and Virtual Environments" (HMI-6) supported by IRIS (Phase 2), the Institute for Robotics and Intelligent Systems part of Canada's National Centers of Excellence program (NCE), and an operating grant "High Performance Robotic Devices" from NSERC, the National Science and Engineering Council of Canada. The second author was supported by a post doctoral fellowship from NSERC during the course of this research.

8 REFERENCES

Bélanger, P. R. (1992). Estimation of angular velocity and acceleration from shaft encoder measurements. *Proc. IEEE Int. Conf. Robotics and Automation,* Nice, France, 1992. pp. 585–592.

Bonneton, B., Hayward, V. (1994). Implementation of a Virtual Wall. Technical Report, Center for Intelligent Machines, McGill University.

Colgate, J. E., Brown, J. M. (1994). Factors affecting the Z-width of a Haptic Display. *IEEE Int. Conf. Robotics and Automation*, pp. 3205–3210.

Corke, P. I., Good M. C. Dynamics Effects in Visual Closed-Loop Systems. (1996). *IEEE T. on Robotics and Automation*, Vol. 12, No. 5, pp. 671–683.

Fagin, S. L. (1964). Recursive linear regression theory, optimal filter theory, and error analysis of optimal system. *IEEE Int. Convention Record*, Vol. 12.

Glad, T., Ljung, L. (1984). Velocity estimation from irregular noisy position measurements. *Proc. IFAC 9th World Congress,* Budapest.

Hayward,, V., Choksi, J., Lanvin, G., Ramstein, C. (1994). Design and Multi-objective Optimization of a Linkage for a Haptic Interface, in *Advances in Robot Kinematics.* J. Lenarcic and B. Ravani (Eds.). Kluwer Academic. pp. 352-359.

Habibullah, B. H., Singh, H., Soo, K. L., Ong, L. C. (1978). A new digital speed transducer. *IEEE Trans. Industrial Electronics and Control Instrumentation,* Vol. IEIC-25, No. 4.

Lewis, F. L. (1986). *Optimal Estimation.* John Wiley and Sons.

Lewis, F. L., Abdallah, C. T., Dawson, D. M. (1993). *Control of Robot Manipulators.* New York: McMillan, 1993.

Minsky, M., Ouh-Young, M., Steele, O., Brooks, F. P. Jr., Behensky, M. (1990). "Feeling and seeing: Issues in force display," *Computer Graphics,* Vol. 24, No. 2.

Rao, M., Xia, Q., Ying, Y. (1993). *Modeling and Advanced Control for Process Industries.* Springer-Verlag.

Sinha, N. K., Szavados, B., di Cenzo, D. C. (1971). New high precision digital tachometer," *Electron. Letters,* Vol. 7.

Sorenson, H. W., Sacks, J. E. (1971). Recursive fading memory filtering. *Information Sciences,* Vol. 3.

Van Valkenburg, M. E. (1960). *Introduction to modern network synthesis.* John Wiley and Sons.